

Electroforming of Large Scale Nickel Structures for Leading-Edge Energy, Aerospace and Marine Applications

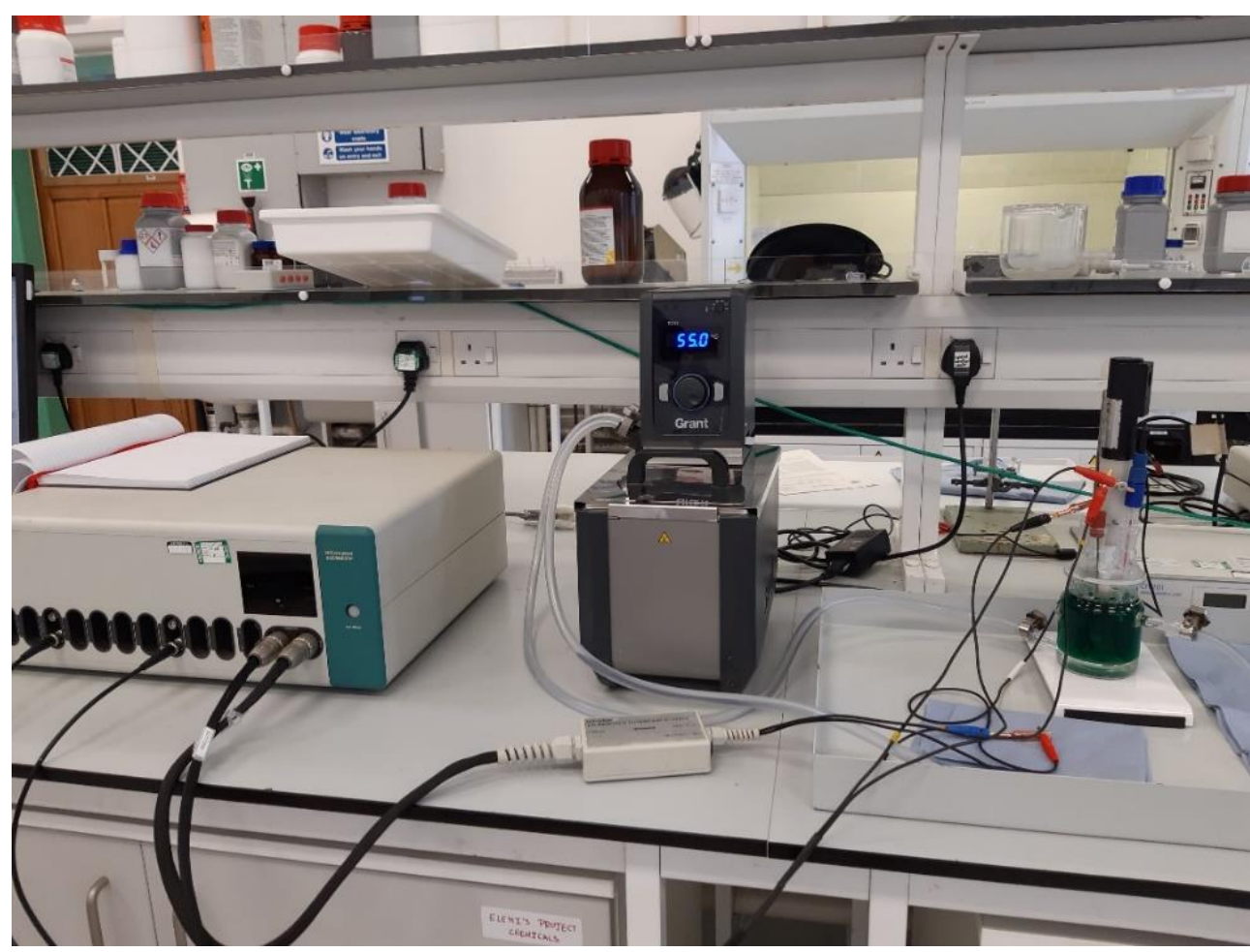
Eleni Andreou¹, Niall Mannion², Steve Wainwright², Sudipta Roy¹

¹ Department of Chemical & Process Engineering, University of Strathclyde, Glasgow, UK
² Doncasters Bramah, part of the Doncasters Group, Sheffield, UK

Electroforming is an electrochemical additive manufacturing process. Some of the strengths of this process include the high energy and resource efficiency coupled with low power consumption. Specifically, nickel electroforming is widely applied in aviation and space industries for the manufacturing of precision, lightweight parts, such as erosion shields. However, as current techniques rely on traditional chemistry and processing methods, utilisation of nickel electroforming remains a specialist activity. Our team aspires to bring the electroforming process to the forefront of AM by opening new horizons for precision manufacturing and overcoming limitations which have rendered specific products “impossible to manufacture” up to this day.

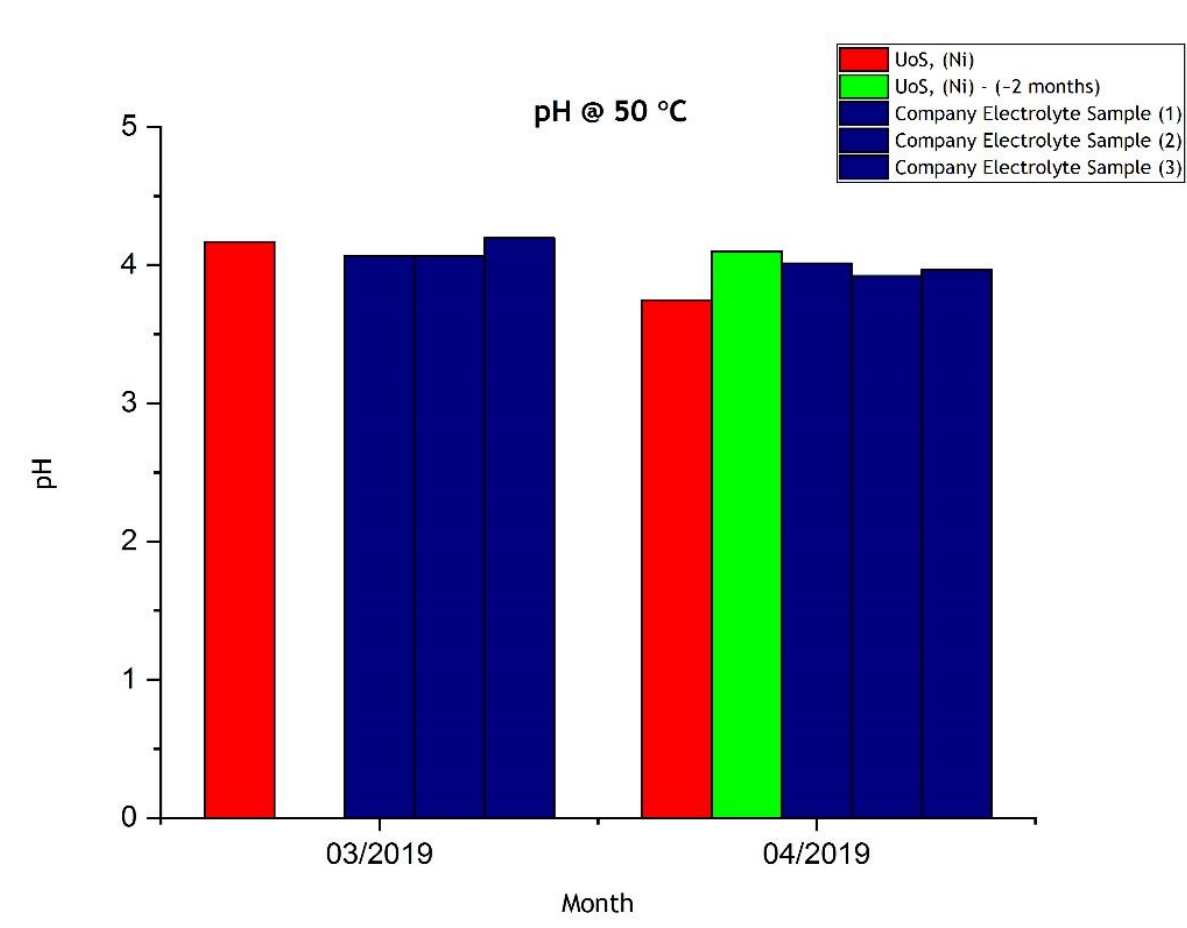
! The first step to do so is the systematic electrochemical analysis and characterisation of the system !

{ Lab Equipment }



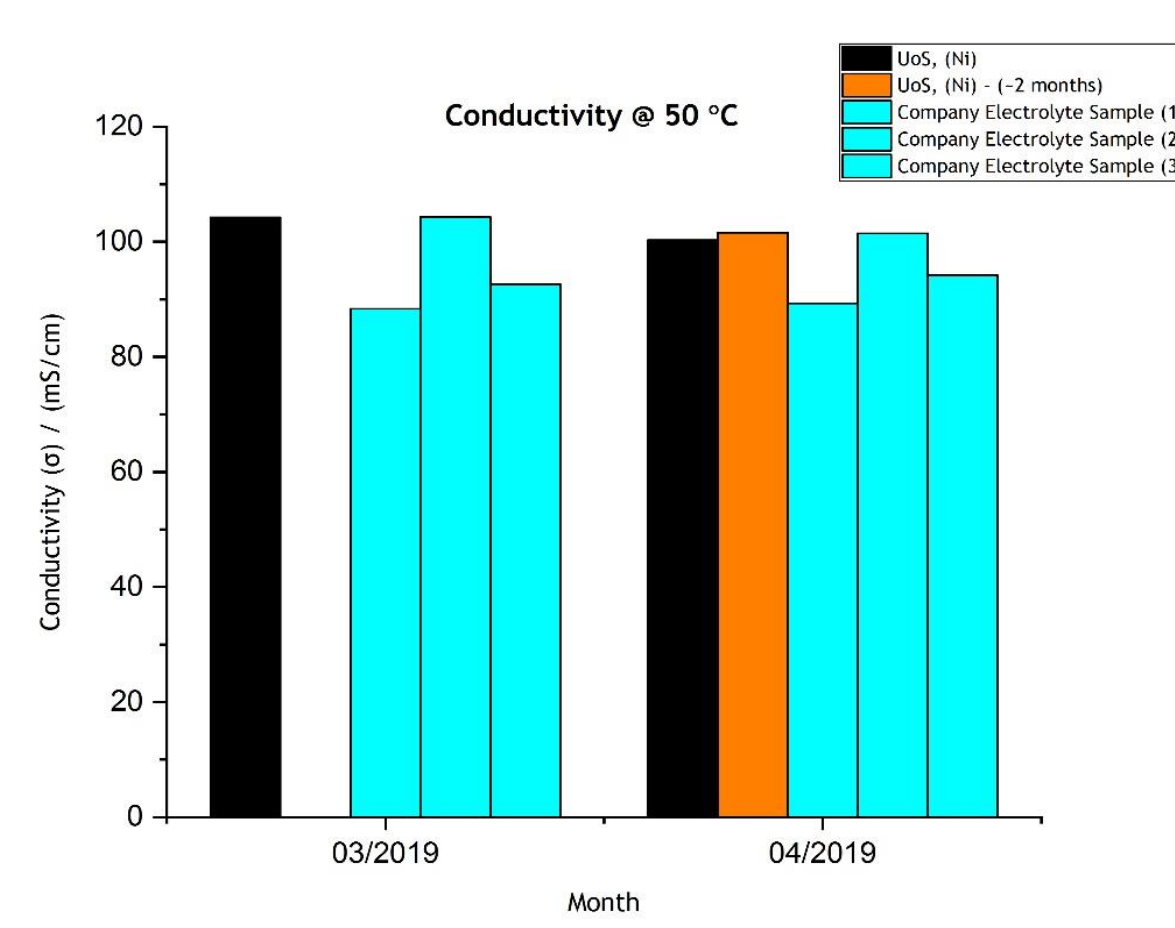
Complete lab setup. (From left to right) Metrohm Autolab Potentiostat/Galvanostat, Water bath, Double-wall Lab Cell, Rotating Disk Electrode (WE), Nickel anode (CE), SCE RE, Stainless Steel Disk Mandrels.

{ pH }



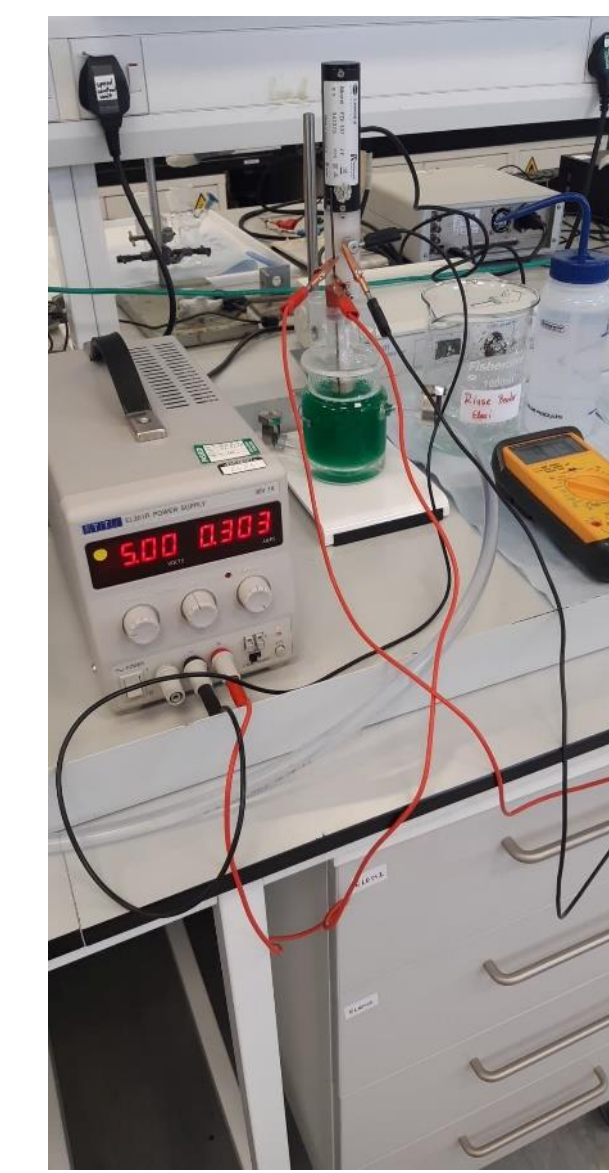
pH = 4 @ 50 °C, in agreement with literature [Y. Tsuru et al., 2002]. Boric acid is a significant stabilising parameter for the solution pH.

{ Conductivity (σ) }



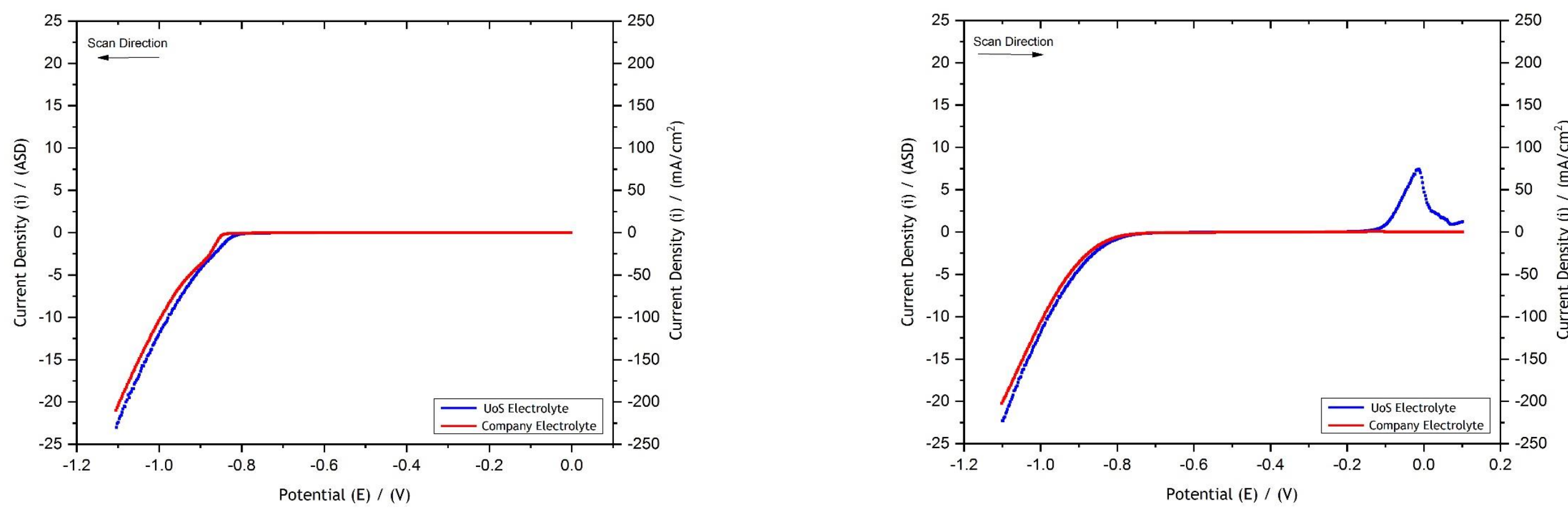
σ ranges between 88 - 104.5 mS/cm @ 50 °C, in agreement with literature [Y. Tsuru et al., 2000]. The excess of nickel in the solutions guarantees stability in conductivity values.

{ Deposition Equipment }



A power supply was used for deposition experiments to represent better the industrial process (current-controlled process). This setup provides us with the ability to measure the WE potential separately via a multimeter and against a SCE RE. The energy that is actually consumed for the primary reactions on the working electrode can, this way, be monitored.

{ Linear Sweep Voltammetry [IR - Corrected Data] }



- ✓ Efficient deposition was determined between 10 - 12 ASD for the pure sulfamate solution.
- ✓ Nickel deposition seems to be “slower” for the company electrolyte sample.
- ✓ Company electrolyte sample seems to be “weaker” than UoS prepared electrolyte.

Experiments with both electrolytes were conducted at 50 °C and 1500 rpm, for 30 min. The resistivity was measured at 4.255 Ω for the UoS electrolyte and 3.941 Ω for the company electrolyte. 80% of each value (3.404 Ω and 3.153 Ω, respectively) was added as input in the NOVA software, during the LSV experiments, to give the IR-corrected data. Current range at 100 mA.

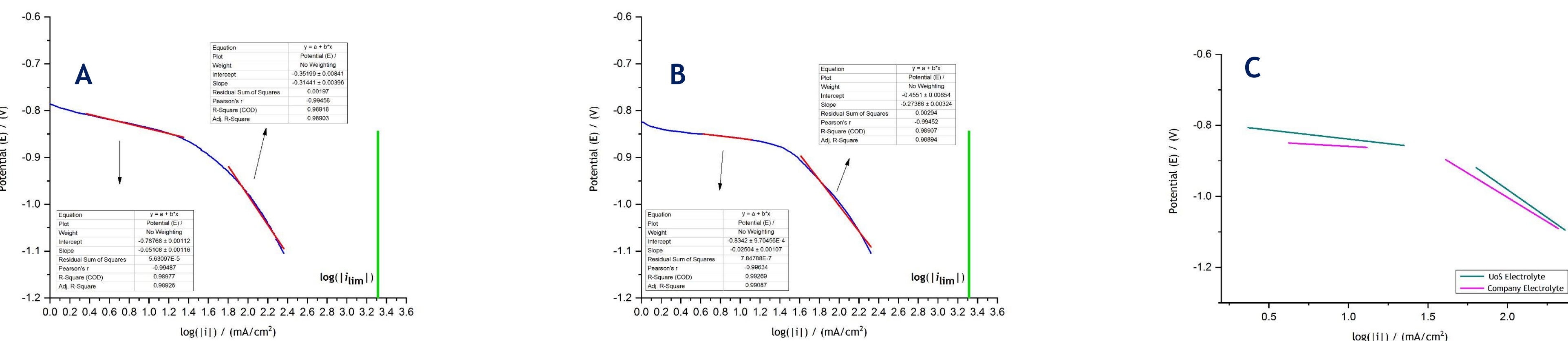
{ Deposition Experiments }

Galvanostatically controlled deposition experiments were carried out and both the total process and working electrode current and potential were measured. The data is used for LSV data correction. Mass balance calculations determine the experiments’ efficiency. Experimental data is gathered at 50 °C, under agitation. All lab results are tested for their reproducibility and compared to the industrial data.

i_{app} (ASD)	Thickness* (μm)	Deposition Rate (mm / h)
42.233	281.56	0.56
19.709	154.18	0.308
3.981	44.46	0.089
1.07	7.3	0.015

Indicative (*) deposit thickness and deposition rate for deposition experiments under various current density values, using the UoS-prepared electrolyte, at 1000 rpm, for 30 min.

{ Tafel Slopes }



A. Tafel slopes for the UoS electrolyte system. OCP = -0.254 V (vs SCE), slope₁: 51 mV/dec (defines a_1^A), slope₂: 314 mV/dec (defines a_2^A).
 B. Tafel slopes for the company electrolyte system. OCP = -0.278 V (vs SCE), slope₁: 25 mV/dec (defines a_1^B), slope₂: 274 mV/dec (defines a_2^B).
 C. Overlap of the A & B slopes.

The two linear areas at each plot may indicate change in the reaction mechanism, as the second linearity appears below the mass transfer limiting current value [$\log(|i_{lim}|) = 3.32 \text{ mA} / \text{cm}^2$]. The second slopes are better comparable than the first ones for each system; this may indicate different starting reaction mechanisms until the system stabilises at its second state. Further investigations are ongoing.

{ Deposits }



The quality of the deposits developed by the use of the UoS-prepared electrolyte was “higher” while, the deposits prepared by the use of the company’s electrolyte sample presented higher dendritic growth. Investigations to determine the reasons for these observations are ongoing.

{ Future Plans }

Detailed investigation on reactor design can provide information on process parameters that affect the properties of final electroformed products. Deposits characterisation will, also, help in this effort and is scheduled for the near future. The simulation modelling of the electroforming process, using COMSOL® software, could open new horizons in increasing the range of the possible geometries, shapes and production volumes that could be electroformed. Working in that direction, a prototype, 40 L electroforming tank is currently under construction and will be accommodated at UoS for in-house experiments that can be compared directly to the industrial process.

$$i_{lim} = \frac{zFD_{eff}}{\delta} \times c_{Ni}$$

z: ions exchanged = 2
 F: Faraday constant = 96485
 D_{eff} : Diffusion coefficient = $5.55 \cdot 10^{-6} \text{ cm}^2 \text{ s}^{-1}$ [Halmdienst et al., 2007]
 c_{Ni} : Nickel concentration in solution = 2.07 M
 δ , electrodes distance: $\delta = 1.61 \times D^{0.3333} \times \nu^{0.1666} \times \omega^{-0.5}$

a_1^A	a_2^A
1.257	0.204
a_1^B	a_2^B
2.564	0.234

$$E_{eq} = E^0 + \frac{0.059}{2} \log[Ni^{2+}]$$

E^0 (vs SCE) / V → $E_{rev} = -0.492 \text{ V}$ (ignoring activity effects)

$$a = \frac{-2.303RT}{a_n F} \times \log i_0$$